Antibacterial Modification of Microcrystalline Cellulose by Grafting Copolymerization

Ying Liu,[a] Lin Li,[a] Xiaolin Li,[a] Yingfeng Wang,[a] Xuehong Ren,[a,*] and Jie Liang [b]

Microcrystalline cellulose (MCC) has the advantage of a high specific surface area as compared to that of conventional cellulose fibers. In this study the monomer methacrylamide (MAM) was used to treat MCC by grafting copolymerization. SEM, FTIR, and solid ^{13}C NMR were used to characterize the morphology and composition of MAM-g-MCC. After the chlorination of MAM-g-MCC with 10% sodium hypochlorite solution, the grafted MCC exhibited antibacterial activity as a result of the formation of N-Cl bonds. The thermal stability, antibacterial ability, and storage stability of chlorinated MAM-g-MCC were also studied. The results showed that the chlorinated MAM-g-MCC had excellent storage stability and could inactivate all S*. aureus* and *E. coli* O157:H7 within 10 min.

Keywords: Microcrystalline cellulose; N-halamine; Methacrylamide; Antibacterial

*Contact information: a: Key Laboratory of Eco-textiles of Ministry of Education, College of Textiles and Clothing, Jiangnan University, Wuxi 214122, Jiangsu, China; b: The Education Ministry Key Lab of Resource Chemistry and Shanghai Key Laboratory of Rare Earth Functional Materials, Shanghai Normal University, Shanghai 200234, China; *Corresponding author: xhren@jiangnan.edu.cn*

INTRODUCTION

Cellulose, one of the most abundant natural materials, has garnered attention in recent decades because of its renewability, biodegradable characteristics, and availability from a variety of sources (de Oliveira Taipina *et al.* 2013). Cellulose is a branched linear polymer with numerous hydrogen bonds. It contains crystalline and amorphous regions and its crystal structure is cellulose I, a mixture of cellulose I-α and I-β in a parallel conformation of two anhydroglucose units joined by β-D glycosidic linkages (Eichhorn and Young 2001). After it is treated with acid, the proportion of amorphous region decreases; cellulose particles can be obtained at the micro- or even the nano-scale *via* acid hydrolysis. Microcrystalline cellulose (MCC), from which the amorphous regions have been partly removed by acid hydrolysis, contains a large amount of cellulose and has the advantage of high specific surface area as compared to that of other conventional cellulose fibers. MCC can easily be modified by monomers and imparted with specific functions. Jiang *et al*. (2012) found that chemical modification of MCC with cyanuric chloride was useful to increase the glucose yield from the hydrolysis of cellulose, making cellulose-based ethanol possible. MCC has also been modified and used as binding material to enhance the compatibility of various substrates (Mathew *et al.* 2005; Petersson and Oksman 2006). However, there have been very few studies of MCC with antibacterial properties.

As one of the most powerful biocides, N-halamine compounds have attracted much interest in recent years given their rechargeability and high efficacy against various microorganisms, including bacteria, viruses, and fungi (Ren *et al*. 2008a; Zhang *et al*. 2013; Zhuo and Sun 2013; Liu *et al.* 2014). N-halamine precursors have structures of

amine, amide, or imide. After halogenation, the nitrogen-hydrogen groups can be oxidized to form nitrogen-halogen groups, which can transfer oxidative halogens to microorganisms' surfaces, destroying their cellular systems and killing the cells (Chen and Sun 2006; Kou *et al*. 2009). Some researchers have proposed that intact chloromelamine moieties may also have biocidal effects, inhibiting the growth of organisms if the free chlorines present in wet environments are not sufficient to inactivate tougher microorganisms (Chen *et al.* 2007). After organisms are inactivated, the oxidizing nitrogen-halogen groups are reduced to nitrogen-hydrogen groups that can be rehalogenated by sodium hypochlorite; the materials modified by N-halamine compounds have long-term antibacterial properties (Sun amd Sun 2001; Zhu *et al.* 2012). Given their ideal antibacterial activity, N-halamine compounds are widely used in surfaces such as fabrics (Lin *et al.* 2001; Liu and Sun 2006; Ren *et al*. 2009a), silica gel (Liang *et al.* 2006; Barnes *et al*. 2007; Cerkez *et al.* 2012), and paints (Cao and Sun 2009; Kocer *et al.* 2011a).

A series of N-halamine compounds have been coated onto the cellulose surface, *via* hydroxyl groups, siloxanes, and epoxides, as tethering groups. 3-(2,3-Dihydroxypropyl)-7,7,9,9-tetramethyl-1,3,8-triazaspiro (4.5) decane-2,4-dione (TTDD diol) was coated onto the cellulose surface with the assistance of 1,2,3,4-butanetetracarboxylic acid (BTCA) as a cross-linking agent (Ren *et al*. 2009b). 3-Glycidyl-5,5-dialkylhydantoins, a copolymer of 3-chloro-2-hydroxypropylmethacrylate and glycidyl methacrylate, and 1-glycidyl-s-triazine-2,4,6-trione containing epoxides, can be coated onto cellulose *via* the traditional finishing method (Liang *et al*. 2007b; Kocer *et al.* 2011b; Ma *et al*. 2013). 3-(3-Triethoxysilylpropyl)-7,7,9,9-tetramethyl-1,3,8-triazaspiro(4.5)decane-2,4-dione, 5,5-dimethyl-3-(3'-triethoxysilylpropyl) hydantoin, and 4-(3-triethoxysilylpropoxyl)-2,2,6,6-tetramethylpiperidine were also bonded to cotton surfaces because of the presence of siloxane groups (Liang *et al*. 2007a; Ren *et al*. 2008b). Among the treatment methods mentioned above, a radical polymerization process was also used to produce antimicrobial cellulose. Acrylamide (AM) and methacrylamide (MAM) were grafted onto cotton by a radical polymerization process, and the treated fabrics provided rapid antibacterial activity against both gram-positive and gram-negative bacteria (Liu and Sun 2006, 2008).

To the best of our knowledge, the modification of MCC by N-halamines has not been previously studied. In this study, MAM was used to modify MCC with N-halamine structures. MAM was grafted onto MCC by radical polymerization and the grafted MCC was characterized by FTIR, SEM, and solid NMR. The thermal stability, antibacterial properties, and chlorine stability towards the storage of the chlorinated MAM-g-MCC were also investigated.

EXPERIMENTAL

Materials

Microcrystalline cellulose (MCC) and methacrylamide (MAM) were purchased from J&K Chemicals, Shanghai, China. Sodium persulfate and other chemicals were purchased from Sinopharm Chemical Reagent Co., Ltd., Shanghai, China.

Fourier transform infrared (FTIR) spectra were obtained using a NICOLET 10 FT-IR spectrometer (Nicolet Instrument Corporation, Madison, WI). A SU 1510 field emission scanning electron microscope (SEM) was used to characterize the surface

morphology of MCC and MAM-g-MCC (Hitachi, Tokyo, Japan). The X-ray diffraction (XRD) patterns of MCC and MAM-g-MCC were detected by a Bruker Instrument model D8 in a 2θ range of 10 to 60° (Bruker AXS, German). Thermo-gravimetric analysis (TGA) was conducted using a thermo-gravimetric analyzer (Q50, TA Instruments, USA).

Grafting MAM onto MCC

MAM and sodium persulfate were mixed in an appropriate ratio into distilled water and stirred for 15 min to obtain a uniform solution. Then, a set amount of MCC was placed in the solution in a 100-mL flask. The reaction was conducted at 60 °C for 5 h. After filtration, the sample was extracted with distilled water for 48 h to remove un-grafted MAM monomers and homopolymers. Then the sample was dried and stored in a desiccator for further study. The grafting yield of MAM modified MCC (MAM-g-MCC) was 11%. And the reaction process is illustrated in Scheme 1.

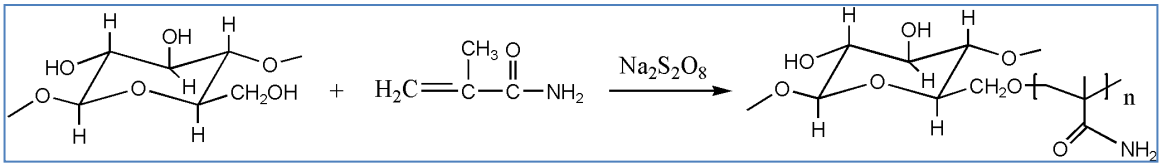

Scheme 1. Reaction process of MCC with MAM

Chlorination and Analytical Titration

MAM-g-MCC samples were soaked in 10% commercial sodium hypochlorite solution at pH 7 during the chlorination process (Liu and Sun 2008). After 60 min, chlorinated MAM-g-MCC samples were filtered and washed with excess distilled water, filtered again, and dried at 45 °C to remove free oxidative chlorine absorbed on the MCC surface. The chlorine loadings on the chlorinated MAM-g-MCC samples were determined *via* the iodometric/thiosulfate titration method and calculated according to the following equation (Chen *et al*. 2007),

$$[Cl] = \frac{35.5}{2} \times \frac{(Vs - Vc) \times 10^{-3} \times N}{Ws} \times 100 \quad (1)$$

where [*Cl*] is the chlorine content of the sample (%), V_s and V_c are the volumes of sodium thiosulfate solution consumed in titration, respectively (mL), N is the normality of the aqueous sodium thiosulfate solution used in the titration (equiv/L), and W_s is the weight of the chlorinated MAM-g-MCC sample (g).

The chlorine contents of the chlorinated MAM-g-MCC sample increased with the increase of grafting yield. However, the antibacterial efficacy might do not show same trend since the efficient antibacterial activity of N-halamines is related to the hydrophobicity of antimicrobial materials after chlorination (Liu *et al*. 2013).

Chlorine Stability during Storage

The chlorinated MAM-g-MCC was tested for the retention of antimicrobial functions under storage conditions by measuring the chlorine loadings of the samples. Chlorinated MAM-g-MCC samples with known chlorine contents were stored in a dark environment at ambient temperature, and the chloride contents were periodically tested throughout the storage period.

Biocidal Efficacy Test

MCC, MAM-g-MCC, and chlorinated MAM-g-MCC samples were challenged with gram-positive bacterium S. *aureus* (ATCC6538P) and gram-negative bacterium E. *coli* O157:H7 (ATCC 11229). Bacterial suspensions with 5.01×10^5 CFU *S. aureus* and 1.82×10^6 CFU *E. coli* O157:H7 were added to phosphate buffer solution containing 0.1 g of tested sample. The mixtures were sonicated, vortexed, and shaken for several minutes. After contact continued for a predetermined duration, sodium thiosulfate solution was used to quench the oxidative chlorine. The quenched samples were diluted several times and the dilute solutions were placed onto agar plates. Two repetitions of each dilution were performed. The plates were incubated at 37 °C for 24 h for final confirmation of the antibacterial activity of the tested samples.

RESULTS AND DISCUSSION

Characterization of the Grafted MCC with MAM

The surface morphologies of MCC and MAM-g-MCC were investigated by SEM. SEM images with magnifications of 500 and 1,000 times are shown in Fig. 1. MAM-g-MCC had a relatively rough surface compared to that of MCC, indicating that MAM monomers were successfully grafted onto the MCC surface by radical polymerization. In addition, the images showed that the microcrystalline cellulose was of micro-scale size, in the range of 50 to 80 μm.

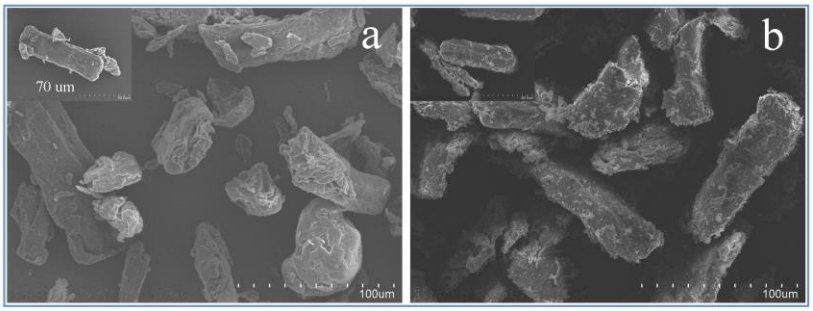

Fig. 1. SEM spectra of MCC with magnification ×500, *inset*: MCC with magnification ×1000 (a); MAM-g-MCC with magnification ×500; *inset*: MAM-g-MCC with magnification ×1000 (b)

Figure 2 shows the FTIR spectra of MCC and chlorinated MAM-g-MCC. Compared to MCC, chlorinated MAM-g-MCC exhibited new peaks at 1,228, 1,690, and 2849 cm^{-1}, which can be attributed to the stretching vibration of the C-N group, the amide band I (C=O), and the C-H vibration of the CH_3 group ascribed to the grafted polymer MAM (Shang *et al*. 2013), respectively. In this study, the C=O band shifted to 1690 cm^{-1} after chlorination, close to the reported position of 1,670 cm^{-1} in the literature (de Santa Maria *et al*. 2003). The shift was attributed to decreased electron density on the nitrogen atom when the amide structure $–C(O)-NH_2$ in the grafted polymer MAM was changed to –C(O)-NHCl, reducing its contribution to the resonance structure $–C(O^-)=N^+HCl$ and consequently increasing the C=O double bond composition by shifting the FTIR band towards higher wavenumber (Liu and Sun 2006). This shift can basically demonstrate the formation of N-Cl bonds after the chlorination reaction. In addition, no significant change was detected for the band located at 3,400 cm^{-1} in either of the two samples, which was mainly assigned to the O-H stretching vibration in the cellulose backbone.

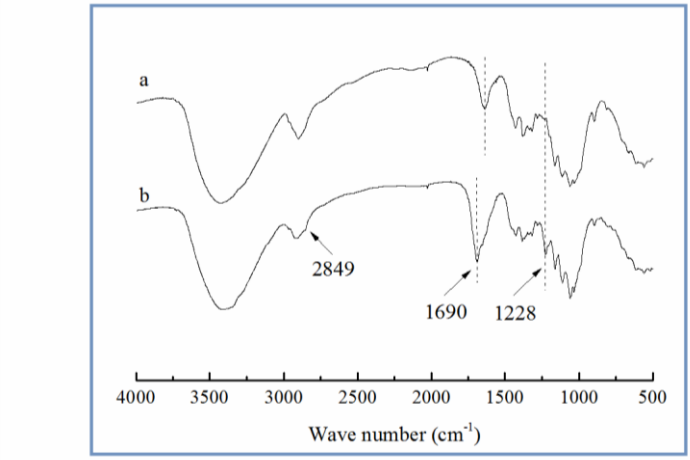

Fig. 2. FTIR spectra of MCC (a) and chlorinated MAM-g-MCC (b)

The ^{13}C NMR spectra of pristine MCC and MAM-g-MCC are presented in Fig. 3. It can be seen that the most intense signals, between 60 and 110 ppm, were those from cellulose backbone carbon atoms. In particular, the signals from 60 to 67, 80 to 92, and 100 to 110 ppm were assigned to C6, C4, and C1, and the signals from 70 to 80 ppm were ascribed to C2, C3, and C5 (Martins *et al.* 2006). The signals at 17, 46, 56, and 183 ppm were assigned to the carbons of the –C-$\underline{C}H_3$ (C9), –$\underline{C}H_2$-C- (C7), -CH_2-$\underline{C}$- (C8), and $\underline{C}$=O(C10) groups, respectively (Shang *et al*. 2013; Altin *et al.* 2014). These signals further confirmed that MAM was successfully chemically bonded to MCC.

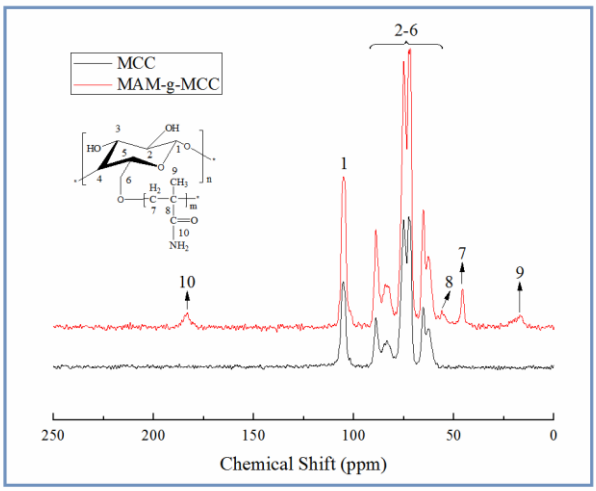

Fig. 3. Solid ^{13}C NMR spectra of MCC and MAM-g-MCC

To observe the crystalline character of MCC and MAM-g-MCC, XRD spectra were detected, and the results are shown in Fig. 4. Both MCC and MAM-g-MCC exhibited typical diffraction peaks at 2θ values of approximately 16°, 22.6°, and 34.6°, and these peaks were assigned to the typical $(1\bar{1}0)$, (110), and (200) planes of cellulose I_β, respectively (Klemm *et al.* 2005; de Oliveira Taipina *et al.* 2013), suggesting that there was no regeneration of crystallinity during the process of grafting MAM onto MCC. The double peak at around 16° indicated that MCC had high cellulose content, and the merging of the two peaks around the 16° region was caused by non-cellulose components (Martins *et al.* 2011; Hossain *et al*. 2012; de Oliveira Taipina *et al*. 2013). Furthermore,

the empirical crystalline degree (I_c) of MCC and MAM-g-MCC was calculated using the Buschle-Diller and Zeronian equation as follows (Buschle-Diller and Zeronian 1992),

$$I_c = 1 - \frac{I_1}{I_2} \quad (2)$$

where I_1 is the minimum amorphous signal intensity at the position $2\theta = 18°$ and I_2 is the intensity associated with the crystalline region of cellulose at position $2\theta = 22.6°$. Based on the XRD analysis, the calculated crystallinity degrees were 82% for MCC and 80% for MAM-g-MCC, suggesting that the crystalline structure of MCC was essentially maintained. No difference was observed in the degree of crystallinity after modification of the cellulose surface, confirming that the modification occurred only at the nanocrystal surface.

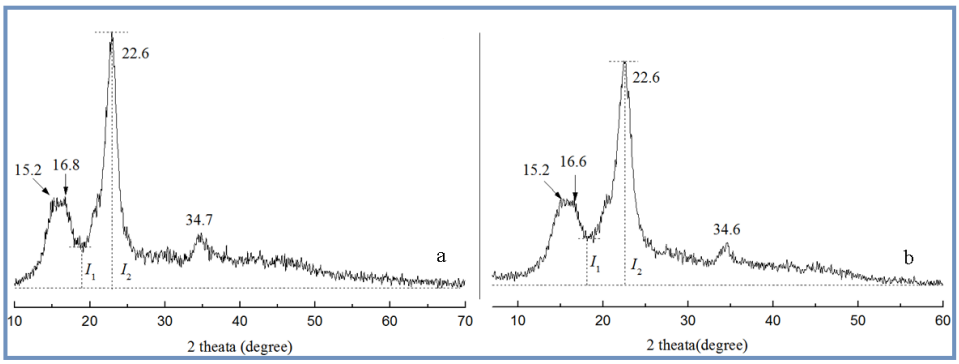

Fig. 4. XRD patterns of MCC (a) and MAM-g-MCC (b)

Thermal Analysis

The thermal stability of pristine MCC, MAM-g-MCC, and chlorinated MAM-g-MCC was investigated by thermogravimetric analysis (TGA), in addition to derivative thermogravimetry analysis (DTG), and the results are presented in Fig. 5. The TGA curve of pristine MCC exhibited two different stages of weight loss. The first stage extended from 40 to 120 °C, and maximum weight loss rate (T_{max}) was at 65 °C, according to the DTG curve. This weight loss corresponded to the volatilization of water adsorbed or bounded on MCC (Li *et al.* 2013). The second stage of weight loss began at 240 °C and was due to the decomposition of the macromolecular chain and the degradation of saccharide rings; T_{max} in this stage was at 351 °C (Chen *et al*. 2011; Liu *et al*. 2014).

The weight loss of MAM-g-MCC was very similar to that of pristine MCC, indicating that the grafting of MAM did not affect the thermal performance of MCC. As for the chlorinated MAM-g-MCC, there was relatively low weight loss at 165 °C as a result of the presence of covalently bound chlorine. The weight of the sample decreased with increasing temperature. The weight loss could be attributed to the degradation of the saccharide rings of MCC and the macromolecule chains carrying N-halamine groups. The T_{max} of chlorinated MAM-g-MCC occurred at 334 °C, which was lower than that of pristine MCC (T_{max} 351 °C) and MAM-g-MCC (T_{max} 341 °C). The decomposition of the N-Cl bond at 180 °C most likely accelerated the thermal decomposition of the cellulose backbone, leading to weight loss from chlorinated MAM-g-MCC at relatively low temperatures (Chen *et al.* 2007).

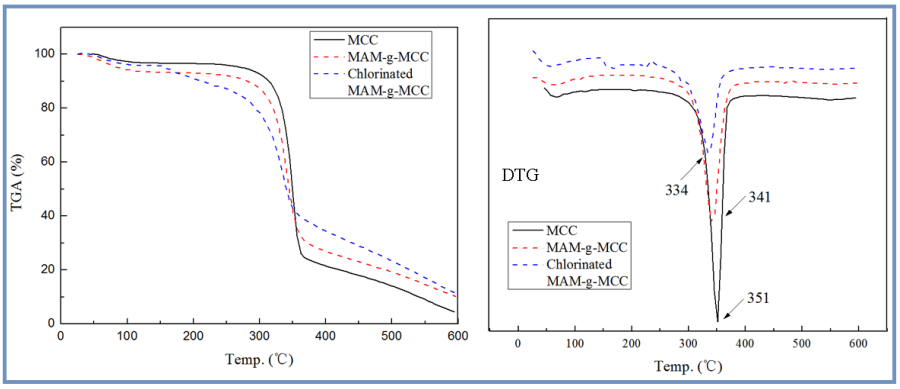

Fig. 5. TGA and DTG curves of MCC, MAM-g-MCC, and chlorinated MAM-g-MCC

Stability during Storage

The storage stability of the chlorinated MAM-g-MCC was tested in a dark environment at ambient temperature, and the results are shown in Table 1. After 90 d of storage, over 60% of the oxidative chlorine was retained and almost all the oxidative chlorine lost could be regained after rechlorination.

Table 1. Chlorine Stability during Storage[a]

Time (d)	[*Cl*] (%)[b]	
	C	R
0	2.98	-
10	2.73	-
20	2.47	-
30	2.31	-
60	2.17	-
90	1.79	2.93

[a] The error in the measured [*Cl*] value was 0.02 %. [b] C, chlorinated before storage test; R, rechlorination after storage test.

Antibacterial Activity

The biocidal efficacies of MAM-g-MCC and chlorinated MAM-g-MCC were tested, and the results are shown in Table 2. The untreated MCC was used as a control. MAM-g-MCC caused small log reductions of *S. aureus* and *E. coli* O157:H7 after 120 min of contact duration. The small log reductions were mainly due to adhesion of the bacteria to the surfaces of MCC and MAM-g-MCC. By contrast, the chlorinated MAM-g-MCC could inactivate 100% of *S. aureus* 5.01×10^5 CFU per sample and *E. coli* O157:H71.82×10^6 CFU per sample within only 10 min of contact duration. The bacterial colonies on the plates are shown in Fig. 6. Clearly, neither MCC nor MAM-g-MCC provided significant antibacterial activity. The chlorinated MAM-g-MCC sample showed that there was no growth of bacteria, both *S. aureus* and *E. coli* O157:H7, after 10 min of contact time. This efficient antibacterial property was due to the oxidative chlorine formed by the chlorination of the N-halamine precursor. The oxidative chlorine was transferred to the cell membrane, reacted with receptors in the cells, and inactivated the microorganisms (Chen *et al*. 2007).

Table 2. Antibacterial Property against *S. aureus* and *E. coli* O157:H7

Sample	Contact time (min)	Bacterial reduction (Log)	
		S. aureus[a]	*E. coli* O157:H7[b]
MCC	120	0.72	0.55
MAM-g-MCC	120	0.90	1.26
Chlorinated MAM-g-MCC $[Cl]$ = 2.87 %	10	5.70	6.26
	30	5.70	6.26
	60	5.70	6.26
	90	5.70	6.26
	120	5.70	6.26

[a]Inoculum: 5.01×10^5 CFU per sample; [b]Inoculum: 1.82×10^6 CFU per sample.

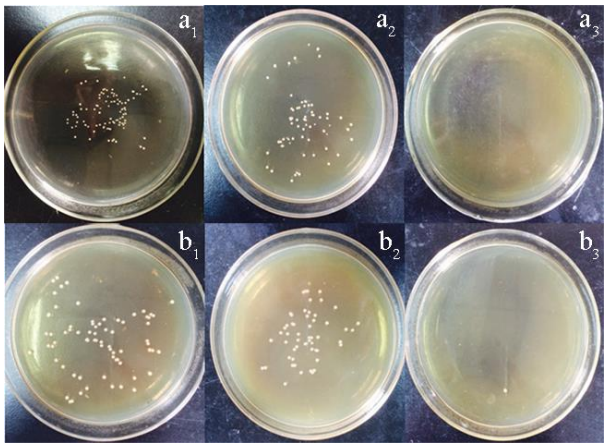

Fig. 6. Photographs of bacterial culture plates of (a) S*. aureus* and (b) E. *coli* O157:H7 after 120 min exposure to tested samples of (1) untreated MCC, (2) MAM-g-MCC, and (3) chlorinated MAM-g-MCC

CONCLUSIONS

1. Methacrylamide was successfully grafted onto the surface of microcrystalline cellulose. The modified microcrystalline cellulose was characterized by SEM, FTIR, solid NMR, and XRD spectra.
2. The results indicated that surface modification by grafting polymerization did not change the degree of crystallinity of the MCC.
3. After chlorination, the modified microcrystalline cellulose became biocidal with good storage stability and could inactivate 100% of *S. aureus* (log reduction 5.70) and 100% of *E. coli* O157:H7 (log reduction 6.26) within 10 min of contact time.
4. The results indicate that antimicrobial, modified microcrystalline cellulose could be used as a potential antibacterial material in water disinfection and healthcare applications.

ACKNOWLEDGEMENTS

This work was supported by the Graduate Student Innovation Plan of the Jiangsu Province of China (KYLX-1142), the Project for Jiangsu Scientific and Technological

Innovation Team, and the research fund from the Science and Technology Department of Jiangsu Province of China (BY2014023-09).

REFERENCES CITED

Altin, A., Akgun, B., Sarayli Bilgici, Z., Begum Turker, S., and Avci, D. (2014). "Synthesis, photopolymerization, and adhesive properties of hydrolytically stable phosphonic acid-containing (meth)acrylamides," *J. Polym. Sci., Part A: Polym. Chem.* 52(4), 511-522. DOI: 10.1002/pola.27025

Barnes, K., Liang, J., Worley, S. D., Lee, J., Broughton, R. M., and Huang, T. S. (2007). "Modification of silica gel, cellulose, and polyurethane with a sterically hindered N-halamine moiety to produce antimicrobial activity," *J. Appl. Polym. Sci.* 105(4), 2306-2313. DOI: 10.1002/app.26280

Buschle-Diller, G., and Zeronian, S. H. (1992). "Enhancing the reactivity and strength of cotton fibers," *J. Appl. Polym. Sci.* 45(6), 967-979. DOI: 10.1002/app.1992. 070450604

Cao, Z., and Sun, Y. (2009). "Polymeric N-halamine latex emulsions for use in antimicrobial paints," *ACS Appl. Mat. Interf.* 1(2), 494-504. DOI: 10.1021/am800157a

Cerkez, I., Kocer, H. B., Worley, S. D., Broughton, R. M., and Huang, T. S. (2012). "N-halamine copolymers for biocidal coatings," *React. Funct. Polym.* 72(10), 673-679. DOI: 10.1016/j.reactfunctpolym.2012.06.018

Chen, S., Chen, S., Jiang, S., Xiong, M., Luo, J., Tang, J., and Ge, Z. (2011). "Environmentally friendly antibacterial cotton textiles finished with siloxane sulfopropylbetaine," *ACS Appl. Mat. Interf.* 3(4), 1154-1162. DOI: 10.1021/am101275d

Chen, Z., Luo, J., and Sun, Y. (2007). "Biocidal efficacy, biofilm-controlling function, and controlled release effect of chloromelamine-based bioresponsive fibrous materials," *Biomaterials* 28(9), 1597-1609. DOI: 10.1016/j.biomaterials. 2006.12. 001

Chen, Z., and Sun, Y. (2006). "N-halamine-based antimicrobial additives for polymers: preparation, characterization, and antimicrobial activity," *Ind. Eng. Chem. Res.* 45(8), 2634-2640. DOI: 10.1021/ie060088a

de Oliveira Taipina, M., Ferrarezi, M., Yoshida, I., and Gonçalves, M. D. (2013). "Surface modification of cotton nanocrystals with a silane agent," *Cellulose* 20(1), 217-226. DOI: 10.1007/s 10570-012-9820-3

de Santa Maria, L. C., Aguiar, M. R. M. P., Guimarães, P. I. C., Amorim, M. C. V., Costa, M. A. S., Almeida, R. S. M., Aguiar, A. P., and Oliveira, A. J. B. (2003). "Synthesis of crosslinked resin based on methacrylamide, styrene and divinylbenzene obtained from polymerization in aqueous suspension," *Eur. Polym. J.* 39(2), 291-296. DOI: 10.1016/S0014-3057(02)00196-9

Eichhorn, S. J., and Young, R. J. (2001). "The Young's modulus of a microcrystalline cellulose," *Cellulose* 8(3), 197-207. DOI: 10.1023/A:1013181804540

Hossain, K. Z., Ahmed, I., Parsons, A., Scotchford, C., Walker, G., Thielemans, W., and Rudd, C. (2012). "Physico-chemical and mechanical properties of nanocomposites prepared using cellulose nanowhiskers and poly(lactic acid)," *J. Mater. Sci.* 47(6), 2675-2686. DOI: 10.1007/s 10853-011-6093-4

Jiang, X., Gu, J., Tian, X., Li, Y., and Huang, D. (2012). "Modification of cellulose for high glucose generation," *Bioresour. Technol.* 104(0), 473-479. DOI: 10.1016/j.biortech.2011.10.091

Klemm, D., Heublein, B., Fink, H.-P., and Bohn, A. (2005). "Cellulose: Fascinating biopolymer and sustainable raw material," *Angew. Chem. Int. Ed.* 44(22), 3358-3393. DOI: 10.1002/anie. 200460587

Kocer, H. B., Cerkez, I., Worley, S. D., Broughton, R. M., and Huang, T. S. (2011a). "N-halamine copolymers for use in antimicrobial paints," *ACS Appl. Mat. Interf.* 3(8), 3189-3194. DOI: 10.1021/am200684u

Kocer, H. B., Cerkez, I., Worley, S. D., Broughton, R. M., and Huang, T. S. (2011b). "Polymeric antimicrobial N-halamine epoxides," *ACS Appl. Mat. Interf.* 3(8), 2845-2850. DOI: 10.1021/am200351w

Kou, L., Liang, J., Ren, X., Kocer, H. B., Worley, S. D., Broughton, R. M., and Huang, T. S. (2009). "Novel N-halamine silanes," *Colloids Surf. A.* 345(1-3), 88-94. DOI: 10.1016/j.colsurfa.2009.04.047

Li, R., Hu, P., Ren, X., Worley, S. D., and Huang, T. S. (2013). "Antimicrobial N-halamine modified chitosan films," *Carbohydr. Polym.* 92(1), 534-539. DOI: 10.1016/j.carbpol.2012.08.115

Liang, J., Barnes, K., Akdag, A., Worley, S. D., Lee, J., Broughton, R. M., and Huang, T. S. (2007a). "Improved antimicrobial siloxane," *Ind. Eng. Chem. Res.* 46(7), 1861-1866. DOI: 10.1021/ie061583+

Liang, J., Chen, Y. J., Ren, X. H., Wu, R., Barnes, K., Worley, S. D., Broughton, R. M., Cho, U., Kocer, H., and Huang, T. S. (2007b). "Fabric treated with antimicrobial N-halamine epoxides," *Ind. Eng. Chem. Res.* 46(20), 6425-6429. DOI: 10.1021/ie0707568

Liang, J., Owens, J. R., Huang, T. S., and Worley, S. D. (2006). "Biocidal hydantoinylsiloxane polymers. IV. N-halamine siloxane-functionalized silica gel," *J. Appl. Polym. Sci.* 101(5), 3448-3454. DOI: 10.1002/app.24346

Lin, J., Winkelman, C., Worley, S. D., Broughton, R. M., and Williams, J. F. (2001). "Antimicrobial treatment of nylon," *J. Appl. Polym. Sci.* 81(4), 943-947. DOI: 10.1002/app.1515

Liu, S., and Sun, G. (2006). "Durable and regenerable biocidal polymers: Acyclic N-halamine cotton cellulose," *Ind. Eng. Chem. Res.* 45(19), 6477-6482. DOI: 10.1021/ie060253m

Liu, S., and Sun, G. (2008). "New refreshable N-halamine polymeric biocides: N-chlorination of acyclic amide grafted cellulose," *Ind. Eng. Chem. Res.* 48(2), 613-618. DOI: 10.1021/ie8007902

Liu, Y., Ma, K. K., Li, R., Ren, X., and Huang, T. S. (2013). "Antibacterial cotton treated with N-halamine and quaternary ammonium salt," *Cellulose* 20, 3123-3130. DOI: 10. 1007/s 10570-013-0056-7

Liu, Y., Liu, Y., Ren, X., and Huang, T. S. (2014). "Antimicrobial cotton containing N-halamine and quaternary ammonium groups by grafting copolymerization," *Appl. Surf. Sci.* 296(0), 231-236. DOI: 10.1016/j.apsusc.2014.01.106

Ma, K. K., Liu, Y., Xie, Z. W., Li, R., Jiang, Z. M., Ren, X. H., and Huang, T. S. (2013). "Synthesis of novel N-halamine epoxide based on cyanuric acid and its application for antimicrobial finishing," *Ind. Eng. Chem. Res.* 52(22), 7413-7418. DOI: 10.1021/ie400122h

Martins, M. A., Forato, L. A., Mattoso, L. H. C., and Colnago, L. A. (2006). "A solid state 13C high resolution NMR study of raw and chemically treated sisal fibers," *Carbohydr. Polym.* 64(1), 127-133. DOI: 10.1016/j.carbpol.2005.10.034

Martins, M., Teixeira, E., Corrêa, A., Ferreira, M., and Mattoso, L. C. (2011). "Extraction and characterization of cellulose whiskers from commercial cotton fibers," *J. Mat. Sci.* 46(24), 7858-7864. DOI: 10.1007/s10853-011-5767-2

Mathew, A. P., Oksman, K., and Sain, M. (2005). "Mechanical properties of biodegradable composites from poly lactic acid (PLA) and microcrystalline cellulose (MCC)," *J. Appl. Polym. Sci.* 97(5), 2014-2025. DOI: 10.1002/app.21779

Petersson, L., and Oksman, K. (2006). "Biopolymer based nanocomposites: Comparing layered silicates and microcrystalline cellulose as nanoreinforcement," *Compos. Sci. Technol.* 66(13), 2187-2196. DOI: 10.1016/j.compscitech. 2005.12.010

Ren, X., Kou, L., Kocer, H. B., Zhu, C., Worley, S. D., Broughton, R. M., and Huang, T. S. (2008a). "Antimicrobial coating of an N-halamine biocidal monomer on cotton fibers via admicellar polymerization," *Colloids Surf., A* 317(1-3), 711-716. DOI: 10.1016/j.colsurfa.2007.12.007

Ren, X. H., Kou, L., Liang, J., Worley, S. D., Tzou, Y. M., and Huang, T. S. (2008b). "Antimicrobial efficacy and light stability of N-halamine siloxanes bound to cotton," *Cellulose* 15(4), 593-598. DOI: 10.1007/s 10570-008-9205-9

Ren, X., Akdag, A., Kocer, H. B., Worley, S. D., Broughton, R. M., and Huang, T. S. (2009a). "N-Halamine-coated cotton for antimicrobial and detoxification applications," *Carbohydr. Polym.* 78(2), 220-226. DOI: 10.1016/j.carbpol.2009. 03.029

Ren, X. H., Akdag, A., Kocer, H. B., Worley, S. D., Broughton, R. M., and Huang, T. S. (2009b). "N-Halamine-coated cotton for antimicrobial and detoxification applications," *Carbohydr. Polym.* 78(2), 220-226. DOI: 10.1016/j.carbpol.2009.03.029

Shang, W., Huang, J., Luo, H., Chang, P., Feng, J., and Xie, G. (2013). "Hydrophobic modification of cellulose nanocrystal via covalently grafting of castor oil," *Cellulose* 20(1), 179-190. DOI: 10.1007/s 10570-012-9795-0

Sun, Y., and Sun, G. (2001). "Novel regenerable N-halamine polymeric biocides. I. Synthesis, characterization, and antibacterial activity of hydantoin-containing polymers," *J. Appl. Polym. Sci.* 80(13), 2460-2467. DOI: 10.1002/app.1353

Zhang, B., Jiao, Y., Kang, Z., Ma, K., Ren, X., and Liang, J. (2013). "Durable antimicrobial cotton fabrics containing stable quaternarized N-halamine groups," *Cellulose* 20(6), 3067-3077. DOI: 10.1007/s 10570-013-0031-3

Zhu, J., Bahramian, Q., Gibson, P., Schreuder-Gibson, H., and Sun, G. (2012). "Chemical and biological decontamination functions of nanofibrous membranes," *J. Mater. Chem.* 22(17), 8532-8540. DOI: 10.1039/C2JM16605D

Zhuo, J., and Sun, G. (2013). "Antimicrobial functions on cellulose materials introduced by anthraquinone vat dyes," *ACS Appl. Mat. Interf.* 5(21), 10830-10835. DOI: 10.1021/am403029w

Article submitted: May 21, 2015; Peer review completed: July 20, 2015; Revised version received and accepted: October 27, 2015; Published: November 19, 2015.
DOI: 10.15376/biores.11.1.519-529